International Conference on Renewable Energies and Power Quality (ICREPQ'18)
Salamanca (Spain), 21th to 23th March, 2018
Renewable Energy and Power Quality Journal (RE&PQJ)
ISSN 2172-038 X, No.16 April 2018

Direct Model Predictive Control Based Mitigation of Harmonics Using Active Power Filter

Venkata Krishna Gonuguntala, Anke Fröbel and Ralf Vick

Chair of Electromagnetic Compatibility
Otto von Guericke University Magdeburg
Universitätsplatz 2, 39106 Magdeburg (Germany)
Phone number: +49 391 6751094, e-mail: venkata.gonuguntala@ovgu.de, anke.froebel@ovgu.de

Abstract. Nowadays, model predictive control (MPC) techniques are gaining attention in the field of power electronics and its applications; due to the advancement of digital controllers. The performance of MPC techniques depends on many factors such as accuracy of the prediction model, optimization criteria, sampling times, etc. Specifically, under large sampling times, it is necessary to extrapolate the reference in order to avoid reference tracking delays. So far, Lagrange method, vector angle method and repetitive prediction method are presented in the literature. However, the influence of these methods on the compensation capabilities of shunt active power filter (SAPF) has not been investigated so far. In this paper, the performance of direct MPC is analysed and compared with hysteresis current control for SAPF application. The impact of extrapolation methods on the compensation capabilities of SAPF is also presented. One of the drawbacks of direct MPC technique is its spread switching frequency behaviour. To avoid this, a modulation method is applied in the control algorithm to operate the SAPF at fixed switching frequency.

Key words

Active harmonic filters, model predictive control, current control, harmonic distortion, power quality.

1. Introduction

Harmonic mitigation is of prime concern for decades; however, the increasing penetration of switched nonlinear systems into the grid demands some advanced solutions for maintaining power quality. Over the years, many flexible AC transmission system devices have been proposed for power quality improvement. Among them, utilization of shunt active power filters (SAPFs) are commonplace in industrial applications. However, the compensation effectiveness of SAPF mainly depends on the accuracy of reference current generation scheme and performance of the controller. Specifically, the reference tracking capabilities of inner current control loop is of vital importance for shunt active filtering, as it can introduce delays and degrade the performance. Therefore, advanced controllers with dynamic reference tracking capabilities are required for this application [1]. Even though model predictive control (MPC) techniques are prevalent in process industries, their introduction into the field of power electronics and its applications has occurred recently. Unlike conventional control techniques, MPC techniques employ the present actuation based on the knowledge of future possible errors, which can be determined using system model. Although this method appears to be simple, employing this technique is computationally demanding [2]. Therefore, advanced digital controllers such as field programmable gate array or digital signal processor are required [3]. MPC offers two control methods for power electronic applications, direct and indirect model predictive control. Among these two methods, direct MPC has obtained more attention from researcher due to its ease of implementation, flexibility, and its adaptability to discrete nature of power electronic systems [4]. This method is also referred to as finite control set MPC in some literature.

This paper presents the compensation capabilities of SAPF using direct MPC technique. The simulation results are presented for steady state and transient conditions. The performance variation of SAPF due to different reference extrapolation methods is also considered. In section II, the mathematical modeling of SAPF is presented. In section III, the principle of operation of direct MPC based active filter controller is explained and the three different reference extrapolation methods which are used for direct MPC technique are presented. The variable switching frequency nature of direct MPC is resolved by introducing a modulation scheme in the cost function, which is presented in section IV. The simulation results are presented in section V and finally the conclusion is drawn in section VI.

2. System Description and Modeling

Fig. 1 represents the generalized circuit configuration of a SAPF used for power conditioning. The nonlinear load present at point of common coupling (PCC) draws non-sinusoidal currents from the grid. In other terms, it injects harmonics into the grid. The main objective of SAPF is to mitigate these unwanted grid current components by injecting compensating currents at PCC. As a result, the power quality of the grid will be improved [5]. In the adopted structure, the voltage source converter (VSC) of SAPF is required to synthesize the compensating currents and the L-type filter is necessary to prevent the propagation of converter switching harmonics into the grid. The capacitor on the DC side of VSC is required for energy exchange during the SAPF operation [6]. However, the average energy exchange between the filter and the grid is zero. The control unit performs the necessary data acquisition and computation tasks, which are required to estimate the compensating current references. Subsequently, using a current controller, it generates gating pulse required to drive the VSC [7].

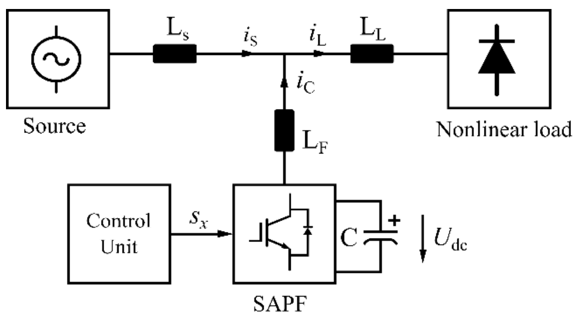

Fig. 1. Generalised block diagram of SAPF.

A. Converter Modeling

The detailed circuit schematics of 2-level, 3-phase VSC along with its Thevenin output impedance is shown in Fig. 2. The VSC is composed of three phase legs and a DC link capacitor. Each phase leg is characterized by two power switches, top and bottom. These switches connect the converter output terminals either to positive (P) or negative DC bus (N), depending on the position of the switch actuated. In a phase leg, the simultaneous operation of top and bottom switch is avoided to limit dc-link shoot through. Since there are three phase legs with two allowed switching states, the total converter switching states will be $2^3 = 8$. Each converter switching state produces a set of phase voltages with respects to positive DC bus terminal, which can be denoted as u_{aN}, u_{bN}, and u_{cN}. Using these voltages, the output voltage space vectors can be defined as

$$\boldsymbol{u}_{\mathrm{SV}} = \frac{2}{3}\left(u_{\mathrm{aN}} + u_{\mathrm{bN}} \cdot e^{j\left(\frac{2\pi}{3}\right)} + u_{\mathrm{cN}} \cdot e^{j\left(\frac{4\pi}{3}\right)}\right) \qquad (1)$$

Since, the converter can be operated in eight switching states, corresponding to them eight voltage vectors ($u_0 - u_7$) can be generated as shown in Fig. 3 [8].

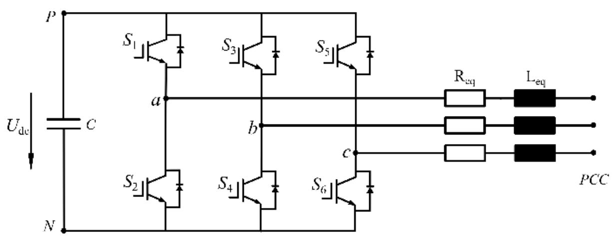

Fig. 2. Voltage Source Converter.

The mathematical model of the SAPF derived from the filter circuit shown in Fig. 2 is

$$\boldsymbol{u}_{\mathrm{PCC}} = \boldsymbol{u}_{\mathrm{xN}} - R_{\mathrm{eq}} \cdot \boldsymbol{i}_{\mathrm{Cx}} - L_{\mathrm{eq}} \cdot \frac{\mathrm{d}\boldsymbol{i}_{\mathrm{Cx}}}{dt} \qquad (2)$$

where, $\mathrm{x} = \mathrm{a, b, c}$. The variable i_{Cx} in (2) represents the compensating current injected into the grid. The converter output parameters (R_{eq} and L_{eq}) represent the Thevenin equivalent impedance (Z_{eq}) at the converter output terminals. These parameters can be determined by the parallel connection of load side (Z_{L}) and grid side (Z_{S}) impedances in series with converter filter impedance (Z_{F}) as follows:

$$Z_{\mathrm{eq}} = \frac{Z_{\mathrm{S}} \cdot Z_{\mathrm{L}}}{Z_{\mathrm{S}} + Z_{\mathrm{L}}} + Z_{\mathrm{F}} \approx Z_{\mathrm{S}} + Z_{\mathrm{F}} \qquad (3)$$

It is assumed that $\boldsymbol{Z}_{\mathbf{L}} \gg \boldsymbol{Z}_{\mathbf{S}}$. Thus, the grid side and filter impedances are sufficient to determine the Thevenin equivalent impedance. Furthermore, to simplify the model, the resistive part of the grid side impedance is neglected, as it has a very little impact on the performance variation [9]. Therefore, the resulting Thevenin equivalent parameters are given as

$$R_{\mathrm{eq}} = R_{\mathrm{F}} \quad \text{and} \quad L_{\mathrm{eq}} = L_{\mathrm{S}} + L_{\mathrm{F}} \qquad (4)$$

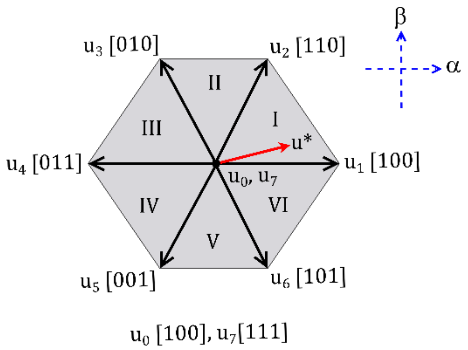

Fig. 3. Converter voltage space vectors.

3. Direct MPC based Active Filter Control

The block diagram of direct MPC based active filter controller (AFC) is shown in Fig. 4. This control approach is basically an online optimization technique, which is designed to be implemented on a digital control platform. Therefore, the control algorithm has to be developed using discrete mathematics. The principal characteristic of direct MPC technique is to use the system model to predict the future values of the controlled variable. Subsequently, the controller uses this information to identify the switching state which results in an optimum performance. The criteria for determining an optimum switching state is defined in the cost function. The implementation of direct MPC based AFC can be realized using four main blocks as follows:

A. Current Reference Generation

The current reference generation is required to maintain the DC link voltage constant and also to extract the unwanted harmonic and reactive power components from the load currents. In this paper, the p-q theory based current reference generation technique has been employed in the controller designing, which can be studied in [10].

B. Prediction Model

In this application, the SAPF model is used to predict the future behaviour. As the digital controllers are being used for these applications, it is necessary to transform the continuous time model into discrete time. Since the model is of first order in nature, the derivate can be sufficiently approximated using forward Euler method [9]:

$$\frac{\mathbf{d}\boldsymbol{x}}{\mathbf{d}\boldsymbol{t}} \approx \frac{\boldsymbol{x}[\boldsymbol{k}+\mathbf{1}]-\boldsymbol{x}[\boldsymbol{k}]}{\mathbf{T_S}} \tag{5}$$

where $\mathbf{T_S}$ is the discretization sampling time. The continuous time model of SAPF can be approximated by substituting (5) in (2). The resultant discrete time model is given in (6). In order to avoid a degradation of compensation performance due to processor computation delay, a two step ahead prediction is necessary. By shifting (6) one step ahead, the prediction model for the second step is obtained as given in (7) [13].

$$\begin{aligned}\hat{\boldsymbol{\imath}}_{\mathbf{Cx}}[\boldsymbol{k}+\mathbf{1}] = \frac{\mathbf{T_s}}{\boldsymbol{L}_{\mathbf{eq}}} \cdot (\boldsymbol{u}_{\mathbf{xN}}[\boldsymbol{k}] - \boldsymbol{u}_{\mathbf{PCC}}[\boldsymbol{k}]) \\ + \left(\mathbf{1} - \frac{\boldsymbol{R}_{\mathbf{eq}} \cdot \mathbf{T_s}}{\boldsymbol{L}_{\mathbf{eq}}}\right) \cdot \boldsymbol{i}_{\mathbf{Cx}}[\boldsymbol{k}]\end{aligned} \tag{6}$$

$$\begin{aligned}\boldsymbol{i}^{\boldsymbol{P}}_{\mathbf{Cx}}[\boldsymbol{k}+\mathbf{2}] = \frac{\mathbf{T_s}}{\boldsymbol{L}_{\mathbf{eq}}} \cdot (\boldsymbol{u}_{\mathbf{xN}}[\boldsymbol{k}+\mathbf{1}] - \boldsymbol{u}_{\mathbf{PCC}}[\boldsymbol{k}+\mathbf{1}]) \\ + \left(\mathbf{1} - \frac{\boldsymbol{R}_{\mathbf{eq}} \cdot \mathbf{T_s}}{\boldsymbol{L}_{\mathbf{eq}}}\right) \cdot \hat{\boldsymbol{\imath}}_{\mathbf{Cx}}[\boldsymbol{k}+\mathbf{1}]\end{aligned} \tag{7}$$

where $\hat{\boldsymbol{\imath}}_{\mathbf{Cx}}[\boldsymbol{k}+\mathbf{1}]$ represents the estimation stage and $\boldsymbol{i}^{\boldsymbol{P}}_{\mathbf{Cx}}[\boldsymbol{k}+\mathbf{2}]$ represents the prediction stage. Using (7), the control algorithm predicts eight converter output current corresponding to eight switching states of the converter.

C. Cost Function Minimization

In order to obtain optimal performance, it is necessary to employ the switching state which produces minimal tracking error. Therefore, at every sampling interval, the eight predicted currents at $[k+2]$ are compared with the reference currents using a cost function $g[k+2]$, as given in (8). The switching state that minimizes the cost function is selected and applied in the next sampling interval [9]:

$$\begin{aligned}g[k+2] = |i_\alpha^*[k+2] - i_\alpha^P[k+2]| \\ + \left|i_\beta^*[k+2] - i_\beta^P[k+2]\right|\end{aligned} \tag{8}$$

where i_α and i_β represent the Clarke components of reference and predicted currents.

D. Reference Extrapolation

In most of the reference tracking applications, it is necessary to have a minimal tracking error. Any larger delay introduced by controller can lead to performance degradation in the corresponding system. Under very high sampling frequencies, f_S (> 50 kHz), it can be assumed that $i^*[k+1] \approx i^*[k]$. This approximation can have a negligible impact on the system performance. However, with smaller sampling frequencies, this approximation leads to considerable tracking delay (one-sample delay). To compensate this delay, it is necessary to consider reference extrapolation [3]. Three widely used extrapolation methods are:

1) Lagrange Method

Considering the fact that the sampling times are constant, it is possible to predict the future values of sinusoidal and non-sinusoidal functions through Lagrange extrapolation. This approach estimates the future value based on the present and past two values of the reference [11]. The n[th] order Lagrange extrapolation is given as follows:

$$\hat{\imath}^*[k+1] = \sum_{l=0}^{n} (-1)^{n-l} \cdot \begin{bmatrix} n+1 \\ l \end{bmatrix} \cdot i^*(k+l-n) \tag{9}$$

Using (9), the third order Lagrange (quadratic) extrapolation for future reference $i^*[k+1]$ is obtained as

$$\hat{\imath}^*[k+1] = 3 \cdot i^*[k] - 3 \cdot i^*[k-1] + i^*[k-2] \tag{10}$$

In this paper, for SAPF application, two-steps ahead reference extrapolation is required to compensate calculation delay, as obtained in (11).

$$\begin{aligned}\hat{\imath}^*[k+2] = 6 \cdot i^*[k] - 8 \cdot i^*[k-1] \\ + 3 \cdot i^*[k-2]\end{aligned} \tag{11}$$

2) Vector Angle Method

Since, it is possible to represent the three phase system variables in an exponential form. This representation of reference variables can be used to estimate the future value by compensating the vector angle change during the sampling interval [11], [12]. An n[th] order reference extrapolation can be obtained as

$$\hat{x}[k+h] = x[k] \cdot e^{jh\omega T_s} \tag{12}$$

where ω is the angular frequency of three phase variables, and h is the prediction horizon length. Using (12), the two-step ahead reference can be estimated as

$$\hat{\imath}^*[k+2] = i^*[k] \cdot e^{j2\omega T_s} \tag{13}$$

3) Linear Prediction with Error Compensation Method

As given in (14), a linear predictor can be used for future reference prediction. However, this approach produces steady state errors (SSE) in the compensation currents. Since, the measured 3-phase quantities are periodic in nature, so the error introduced through linear predictor is also periodic in nature. Thus, the SSE can be eliminated by using repetitive error compensator, which results in an improved prediction of future reference [13]. The block diagram of linear predictor with error compensator is shown in Fig. 5.

$$i_{ref}[k+2] = 1.5 \cdot i_{ref}[k] - 0.5 \cdot i_{ref}[k-1] \tag{14}$$

The principle of this method is to measure the error caused due to linear prediction in the first cycle and eliminate this error in the next cycle. The detailed study on this technique is presented in [13].

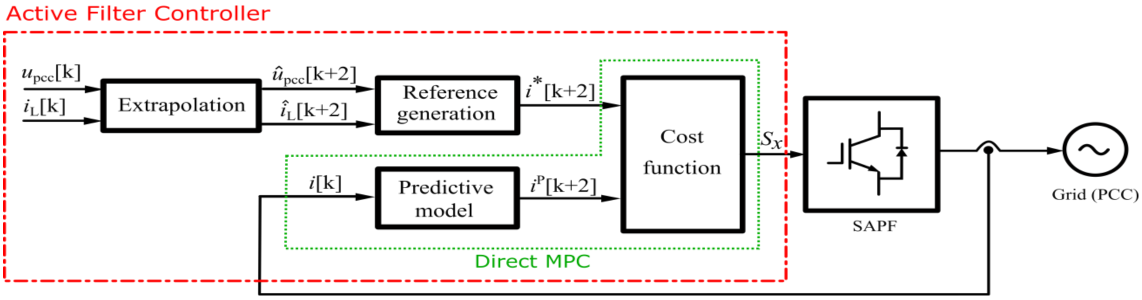

Fig. 4. Direct MPC based active filter controller block diagram.

The two-step ahead $[k+2]$ reference prediction is estimated as follows:

$$\hat{x}[k+2] = [1.5 \cdot x[k] - 0.5 \cdot x[k-1]] + \{x[k+2-N] - [1.5 \cdot x[k-N] - 0.5 \cdot x[k-N-1]]\} \tag{15}$$

where, x can be current or voltage. In Fig. 5, w is the linear prediction of x and d is the error compensation value.

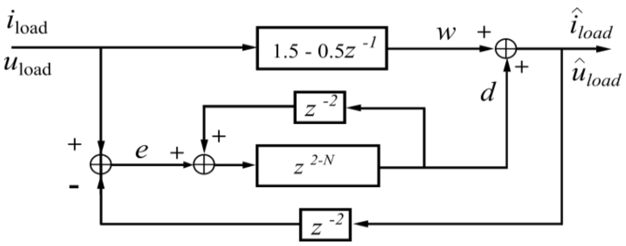

Fig. 5. Linear predictor with repetitive error compensator (according to [13]).

4. Modulated Model Predictive Control

The main advantage of direct MPC is its capability to control multiple variables in a single control loop, instead of cascaded control loops. However in case of direct MPC, the controlled variables exhibit higher ripple due to the lack of modulator and limited number of converter switching states. Moreover, the resulting spectrums of the controlled variables are spread over the frequency range [1], [14]. In order to avoid these drawbacks, a cost function based modulation scheme has been proposed in [1]. This scheme retains all the desired characteristics of direct MPC; meanwhile, it operates the VSC at fixed switching frequency. In this control approach, at every sampling interval, the cost function identifies an optimal sector instead of an optimal switching state. The cost function required to determine the sector is given as:

$$g_{sect}[k+2] = d_0 \cdot g_0 + d_1 \cdot g_1 + d_2 \cdot g_2 \tag{16}$$

where g_i with i = 0, 1, 2 are the cost functions calculated for the voltage vectors (two active and one zero) of the sector. Similarly d_i with i = 0, 1, 2 are the duty cycles corresponding to these voltage vectors. Assuming the duty cycles are inversely proportional to their cost functions as given in (17), where K is a normalized constant to be determined. By solving (17), the expression for the duty cycles is obtained as given in (18).

$$d_0 = K/g_0 \qquad d_1 = K/g_1 \qquad d_2 = K/g_2 \qquad d_0 + d_1 + d_2 = T_S \tag{17}$$

$$\begin{aligned} d_0 &= T_S \cdot g_1 \cdot g_2/(g_0 \cdot g_1 + g_1 \cdot g_2 + g_0 \cdot g_2) \\ d_1 &= T_S \cdot g_0 \cdot g_2/(g_0 \cdot g_1 + g_1 \cdot g_2 + g_0 \cdot g_2) \\ d_2 &= T_S \cdot g_0 \cdot g_1/(g_0 \cdot g_1 + g_1 \cdot g_2 + g_0 \cdot g_2) \end{aligned} \tag{18}$$

At every sampling time, for each sector, the cost functions are evaluated and their corresponding duty cycles values are estimated using (18). Then the optimum sector is identified by minimizing the sector cost function (16). The corresponding duty cycles are employed on VSC in the next sampling interval. In order to reduce the converter harmonics, a symmetrical switching patter for optimal voltage vectors is considered.

5. Simulation Results

A simulation model of the SAPF with the parameters in Table I has been implemented in MATLAB/Simulink. The model was solved by using ODE5 fixed step solver with a step size of $1\mu s$. The proposed direct MPC control algorithm was programmed in S-function block, which facilitates the simulation of discrete time models. In the model, a three-phase diode bridge rectifier driving a RL load is considered as a nonlinear load. The primary control objective of SAPF is to maintain the DC link voltage at its reference while mitigating the harmonics introduced by nonlinear load.

Table I. - Simulation Parameters.

Description	Value	Description	Value
Source voltage ($\boldsymbol{u}_s$)	400 V	Filter Inductor (L_F)	3 mH
Source frequency (f)	50 Hz	Load resistance (R_L)	25 Ω
DC link voltage (u_{dc})	700 V	Load inductance (L_L)	20 mH
DC capacitor (C_{dc})	1000 μF	Sampling time (T_S)	40 μs

A. Steady-State and Transient Analysis

Fig. 6 shows the harmonic mitigation capabilities of SAPF under steady-state and transient conditions. Until $t = 20\ ms$, the nonlinear load draws non-sinusoidal currents from the grid. The compensation currents ($\boldsymbol{i}_{Cx}$) injected by the filter are zero, as it is not connected yet and there is a small decrease in the DC link voltage due to capacitor self-discharge. However, at $t = 20\ ms$, the SAPF is connected to the PCC. From then onwards, the filter injects the compensation currents (i_{Ca}, phase-a) required to mitigate the harmonics introduced by nonlinear load. Thereupon, the grid currents turn sinusoidal. During this period, the PI controller used for DC voltage regulation maintains the DC link voltage at its reference (700 V) with a steady-state error of 0.57 %. The total harmonic current distortion of the source has been reduced from 25.02 % to 3.69 %.

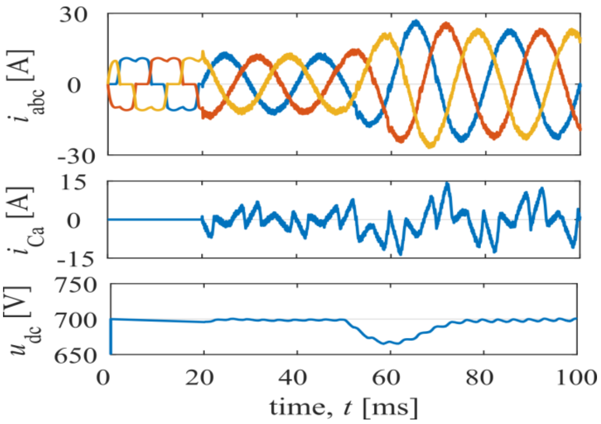

Fig. 6. Simulation results during steady state and transient conditions.

In order to analyse the transient performance of SAPF, at $t = 50\ ms$, the nonlinear load is increased by a factor of two. It is evident from the Fig. 6 that, in spite of the load variation, the proposed control algorithm was effective in compensating the unwanted load harmonic without any delay. The simulation results of instantaneous active (P) and reactive power (Q) are shown in Fig. 7 (a). After $t = 20\ ms$, the unwanted oscillating real power ($\tilde{p}$) and reactive power drawn from the grid are almost completely nullified. Even during transient conditions at $t = 50\ ms$, the proposed controller is still effective in compensating the unwanted power components by injecting the appropriate compensating currents at PCC. The compensating power, which is required to address the VSC losses and also to mitigate the oscillating real power, is shown in Fig. 7 (b). The glitch in P_{comp} at $t = 20\ ms$ is due to prediction error imposed by the reference extrapolation method. After the first cycle, this error will reduce drastically as the error correction data for the second cycle will be available from the first cycle.

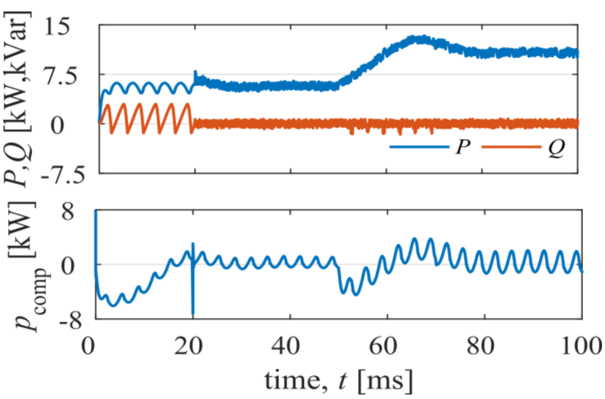

Fig. 7. Instantaneous active and reactive powers (top), compensating real power (bottom).

B. *Performance Comparison with Hysteresis Control*

In order to provide a fair comparison, the performances of both controllers were evaluated under similar operating conditions. One of the common aspects for both direct MPC and hysteresis control is its variable switching frequency. For comparison, the average switching frequency (F_{SW}) of both controllers were maintained at 4 kHz. It is evident from Fig. 8, the compensating current reference (i^*_{Ca}- black) tracking capabilities of direct MPC is much better that hysteresis control. Consequently, the total harmonic distortions of grid current (phase-a) were 3.69% for direct MPC and 4.86% for hysteresis control.

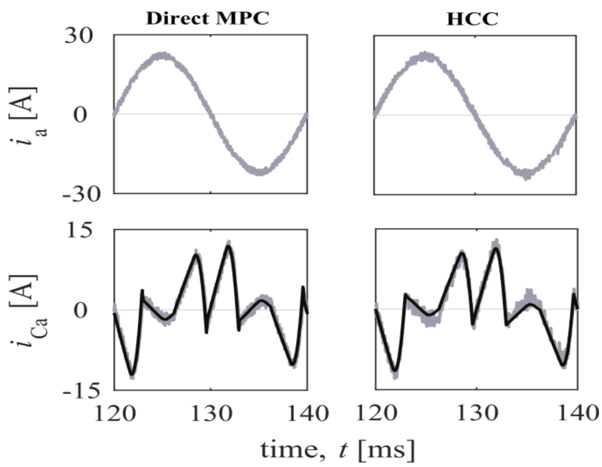

Fig. 8. Comparison of reference tracking capabilities.

C. *Impact of extrapolation methods*

The total harmonic distortion (THD) of source current and the absolute tracking error of compensating current are chosen as the performance indices to evaluate the impact of extrapolation methods. The results in Table II present the influence of extrapolation methods on the compensation performance. It is evident from Fig. 9 (a), the Lagrange method introduces steady-state errors, consequently, there is an increase in absolute tracking error. Fig. 9 (b) appears to be the perfect solution. However, due to the non-sinusoidal load currents, the vector angle method introduces additional error, which can degrade the performance. Even though, the repetitive predictor method needs one fundamental cycle to provide error compensation, but still, it provides the excellent overall performance when compared to the other two methods.

D. *Total Harmonic Distortion*

As explained earlier, the variable switching frequency behaviour of direct MPC method results in a distributed spectrum of the controlled variables, thereby affecting the power quality. From Fig. 10 (top), it is evident that the harmonic spectrum of grid current (phase-a) is distributed over the frequency range wherein it is complex to identify the switching frequency of SAPF. However, in order to attain fixed switching frequency operation, the cost function based modulation scheme was incorporated in the direct MPC control algorithm. It is evident from Fig. 10 (bottom) that the harmonic spectrum of the grid current (phase-a) resulted in a concentrated spectrum with a switching frequency of 25 kHz.

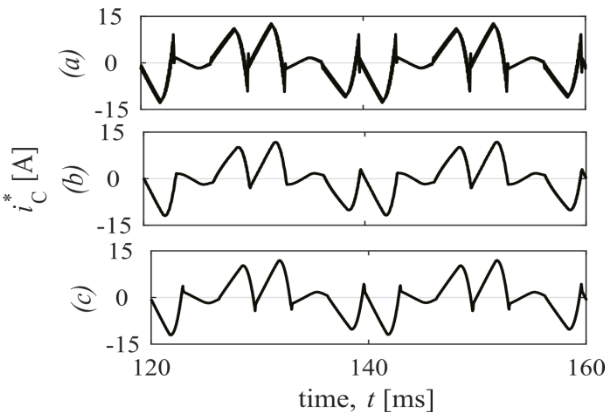

Fig. 9. Compensating reference current by using (a) Lagrange, (b) vector angle, (c) repetitive-predictor method.

Table II. – Comparison of Extrapolation Methods

Methods	**THD$_i$ (Phase-a)**	**Absolute Reference Tracking Error (A)**
Lagrange method	4.23 %	1.3141
Vector angle method	5.36 %	0.5998
Repetitive prediction	3.69 %	0.7646

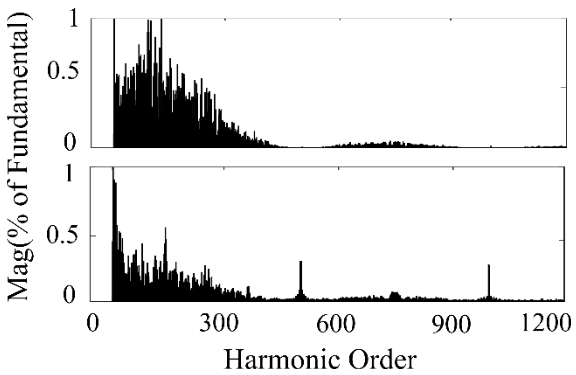

Fig. 4. Harmonic spectrums of grid current for direct MPC (top) and modulated MPC (bottom).

6. Conclusion

In this paper the direct MPC based active filter controller is presented for shunt active power filtering application. The use of direct MPC technique for inner current control loop provided an efficient reference tracking response under steady state and transient conditions. The presented simulation results demonstrate that the direct MPC technique can be a viable alternative for conventional control techniques. Moreover, the effort is put forth to analyse the impact of extrapolation methods on the control performance. The drawback of variable switching frequency has been resolved by implementing a modulation scheme in the control algorithm. The simulation results verify the compensation capabilities of shunt active power filter, the THD of grid current has been reduced from 25.02 % to 3.69 %. The performance variation due to parameter error is in the future scope.

References

[1] L. Tarisciotti *et al.*, "Model Predictive Control for Shunt Active Filters With Fixed Switching Frequency," in *IEEE Transactions on Industry Applications*, vol. 53, no. 1, pp. 296-304, Jan.-Feb. 2017.

[2] K. Antoniewicz and K. Rafal, K “Model predictive current control method for four-leg three-level converter operating as shunt active power filter and grid connected inverter,” in *Bulletin of the Polish Academy of Sciences Technical Sciences*, vol. 65, no. 5, pp. 601-607, Oct. 2017.

[3] P. Cortes, J. Rodriguez, C. Silva and A. Flores, "Delay Compensation in Model Predictive Current Control of a Three-Phase Inverter," in *IEEE Transactions on Industrial Electronics*, vol. 59, no. 2, pp. 1323-1325, Feb. 2012.

[4] S. Kouro, M. A. Perez, J. Rodriguez, A. M. Llor and H. A. Young, "Model Predictive Control: MPC's Role in the Evolution of Power Electronics," in *IEEE Industrial Electronics Magazine*, vol. 9, no. 4, pp. 8-21, Dec. 2015.

[5] A. Fereidouni, M. A. S. Masoum and K. M. Smedley, "Supervisory Nearly Constant Frequency Hysteresis Current Control for Active Power Filter Applications in Stationary Reference Frame," in *IEEE Power and Energy Technology Systems Journal*, vol. 3, no. 1, pp. 1-12, March 2016.

[6] T. Mannen and H. Fujita, "Dynamic Control and Analysis of DC-Capacitor Voltage Fluctuations in Three-Phase Active Power Filters," in *IEEE Transactions on Power Electronics*, vol. 31, no. 9, pp. 6710-6718, Sept. 2016.

[7] H.Akagi, “Modern Active Filters and Traditional Passive Filters,” in *Bulletin of the Polish Academy of Sciences Technical Sciences*, vol. 54, no. 3, pp. 255-269, 2006.

[8] J. Rodriguez *et al.*, "State of the Art of Finite Control Set Model Predictive Control in Power Electronics," in *IEEE Transactions on Industrial Informatics*, vol. 9, no. 2, pp. 1003-1016, May 2013.

[9] P. Acuña, L. Morán, M. Rivera, J. Dixon and J. Rodriguez, "Improved Active Power Filter Performance for Renewable Power Generation Systems," in *IEEE Transactions on Power Electronics*, vol. 29, no. 2, pp. 687-694, Feb. 2014.

[10] E. H. Watanabe, M. Aredes, J. L. Afonso, J. G. Pinto, L. F. C. Monteiro and H. Akagi, "Instantaneous p–q power theory for control of compensators in micro-grids," *2010 International School on Nonsinusoidal Currents and Compensation*, Lagow, 2010, pp. 17-26.

[11] O. Kukrer, "Discrete-time current control of voltage-fed three-phase PWM inverters," in *IEEE Transactions on Power Electronics*, vol. 11, no. 2, pp. 260-269, Mar 1996.

[12] V. Yaramasu, "Predictive control of multilevel converters for megawatt wind energy conversion systems," Ph.D. dissertation, Dept. Electrical &. Computer Eng., Ryerson University, Ontario, Canada, 2014.

[13] M. Vatani, M. Hovd and M. Molinas, "Finite Control Set Model Predictive Control of a shunt active power filter," *2013 Twenty-Eighth Annual IEEE Applied Power Electronics Conference and Exposition (APEC)*, Long Beach, CA, USA, 2013, pp. 2156-2161.

[14] M. Rivera *et al.*, "A modulated model predictive control scheme for a two-level voltage source inverter," *2015 IEEE International Conference on Industrial Technology (ICIT)*, Seville, 2015, pp. 2224-2229.